Relativistic Model for Pion-nucleon Scattering

by

Joe Y. Haskian

TABLE OF CONTENTS

LIST OF FIGURES

LIST OF TABLES

SELF-CONSISTENT RELATIVISTIC MODEL FOR PION-NUCLEON SCATTERING

1. INTRODUCTION

For decades nuclear physicists have been attracted to the pion-nucleon interaction [1,2]. The reason is twofold: the knowledge of π-nucleon interaction comprises the foundation for any dynamical theory of nuclei and this knowledge provides clues to the understanding of the internal structure of hadrons.

The interaction of low and intermediate-energy pions with nucleons is dominated by the resonant amplitude for exciting the nucleon to its spin-3/2, isospin-3/2 excited state $\Delta(1232)$. This physical state is a mixture of an "elementary" delta composed of 3 valence quarks, coupled to the nucleon-pion states. To describe pion-nucleon scattering in terms of effective hadronic degrees of freedom, the physical delta has to be constructed by dressing the "elementary" delta. In this paper we construct a covariant, causal, crossing-symmetric model for the non-local effective interactions of pions, nucleons and deltas, and obtain accurate fits to observed amplitudes for pion-nucleon scattering.

To apply field theory to hadrons, two difficulties of principle have to be faced: regularizing ultraviolet infinities, and choosing a non-perturbative scheme of successive approximations. The short-distance infinities arise because we must dress the delta with a self-energy loop expressing its decay into a pion-nucleon two-body state. We apply the method of Siemens et al. [3] to regulate loop integrals by invoking the internal structure of the hadrons, which smears their interactions over a distance of a few tenths of a fermi. This smearing of the emission/absorption vertex Γ has to be implemented in a way which preserves causality and unitarity. An adequate technique is derived in [3] and applied to a simplified model in [4]. Here we exploit this technique in a quantitative phenomenology of low-energy pion-nucleon interactions.

Since the scattering of low-energy hadrons is caused by strong interactions, we also need a phenomenology suitable for non-perturbative systems. Our guiding principle is to consider explicitly only transitions to single-particle intermediate states, which lead to poles in the two-body scattering matrix T. Crossing symmetry

requires that these poles have to be used in all channels in which they appear. It is well known that these single-particle processes are not sufficient to describe the two-body scattering; for example they do not by themselves lead to unitary on-shell amplitudes. Multiple-scattering processes involving intermediate states with two or more particles are therefore essential. Fortunately these more complicated processes are expected to have a smooth dependence on the momenta of the scattered particles, because their contributions to T can be represented by dispersion integrals over the two- and more-body phase space of intermediate states [5,6]. Thus we choose to parametrize them by smooth functions of the kinematic variables, employing functional forms like those used for smearing the three-field vertices Γ appearing in the self-energy loops. This approximation could be improved by explicit inclusion of 2- or more-particle intermediate states, which would require solving integral equations [6].

We develop this method in Section 2 for low-energy pion-nucleon scattering, which allows us to illustrate the principles and techniques. In Section 3 we describe our phenomenological fits to pion-nucleon scattering data, which allow us to determine the strong-interaction vertices. Finally in Section 4 we summarize our results and draw conclusions for future work.

2. THEORETICAL FRAMEWORK

Our aim is to describe the pion-nucleon system through the energy range of the $\Delta(1232)$ resonance. Because of the width of the Δ, this region goes up to about 1400 MeV in the πN center-of-mass energy $\sqrt{s}$. In this range the relative momentum is less than 1.5 fm^{-1}, so phase shifts with orbital angular momentum L=0 and 1 are needed. Coupling the isospin and angular momentum of the nucleon to those of the pion, 6 amplitudes T_{LIJ} are needed for total angular momentum $J\times$ 2 and total isospin $I\times 2$: LIJ = S11, S31, P11, P13, P31 and P33. Even though the main many-body physics is in the P33 channel, we want to be sure we have an adequate description of the other channels as well since crossing symmetry links them, and since a pion in the interesting energy range will experience all these interactions. Describing these channels requires degrees of freedom beyond the N, π and Δ that are our main interest.

Formally we begin by separating the connected 4-field vertex T into its 1-particle reducible part T^{1PR} and the irreducible remainder, the proper vertex T^{1PI} :

$$T_{LIJ} = T^{1PR}_{LIJ} + T^{1PI}_{LIJ} \tag{2.1}$$

The 1-particle reducible part in turn consists of the three contributions shown in Figure 2.1., corresponding to whether the intermediate 1-particle state is in the s, t, or u channel; dashed and solid lines are dressed boson and fermion propagators, respectively, and shaded triangles represent the proper three-point vertex G. The nature of these contributions to T^{1PR}_{LIJ} varies with their kinematics.

The s-channel pole is evaluated at the total c.m. energy of the πN system, leading to resonant behavior when this energy approaches the mass of the intermediate particle, which has to carry the baryon number and other quantum numbers (LIJ) of the initial scattering state. The u-channel pole is evaluated at an energy $\sqrt{u}$ which is less than the nucleon mass; since it also must carry baryon number, the intermediate state has to be a baryon, which is virtual since its 4-momentum squared is less than the mass squared of the lowest baryonic state. The t-channel pole is also below its mass shell, since the 4-momentum transfer t is spacelike; there is no baryon number in this channel, so the exchanged particle must be a meson, of which the lowest-mass candidate is the ρ meson. The momentum transfers t and u depend on the πN scattering angle, so that each exchanged particle contributes

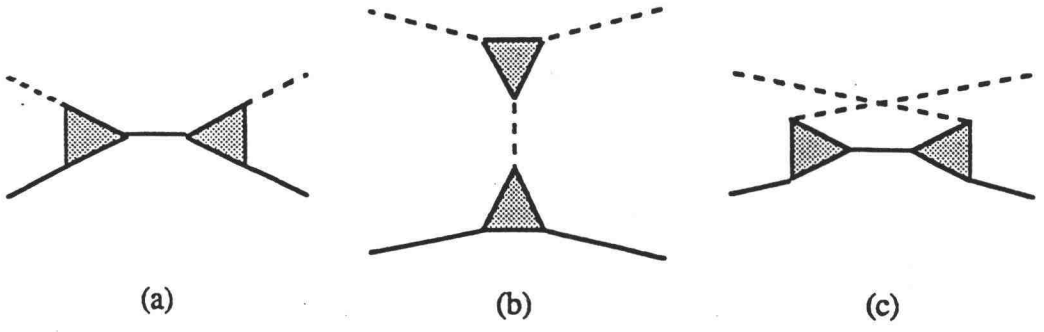

Figure 2.1. Pole contributions to the πN scattering amplitude: (a) s channel; (b) t channel, (c) u channel.

to several angular momentum channels LIJ. However the fact that the t and u channel poles are off mass shell allows us to expect that their contributions to the T matrix will be smooth functions of the c.m. energy, unlike the resonant s-channel amplitudes. We may also hope that they may be smaller than the on-shell resonant amplitudes, which we expect to approach the limit imposed by partial-wave unitarity.

Since the separation into $T^{1PR}_{LIJ} + T^{1PI}_{LIJ}$ is topological, all the propagators and vertices are fully dressed [3,4]. This means that many rescattering processes are already included in T^{1PR}_{LIJ}. Figure 2.2 shows some examples of rescattering processes which correspond to dressing the propagators and vertices of Figure 2.1(a). It is important to note that these contributions include the largest part of the scattering, the s-channel pole, which therefore cannot contribute to multiple scattering processes. As a result, we expect the irreducible part T^{1PI}_{LIJ} to be small. Our phenomenological analysis will confirm this expectation.

In addition to the contributions from single-particle intermediate states shown in Figure 2.1, the scattering matrix T includes 1-particle irreducible contributions T^{1PI}_{LIJ} from 2- and more-particle intermediate states, and perhaps also from multiquark states not included in the low-energy hadronic model. Some examples of processes contributing to T^{1PI}_{LIJ} are shown in Figure 2.3. These processes represent rescattering, and could be included by solving integral equations of the Bethe-Salpeter and Lippmann-Schwinger type [6]. However, we expect the results

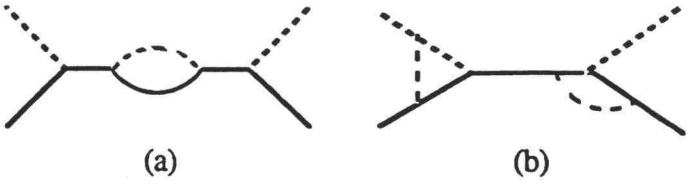

Figure 2.2. Some multiple-scattering contributions to the 1PR πN scattering amplitude: (a) included in dressed propagator; (b) included in dressed vertex.

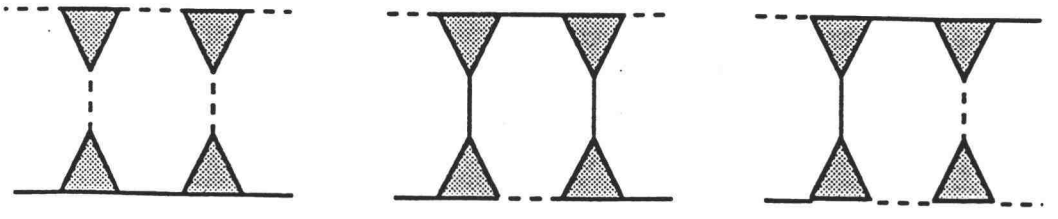

Figure 2.3. Some contributions to the 1PI πN scattering amplitude from rescattering with 2-particle intermediate states.

for T^{1PI}_{LIJ} to be smooth functions of the kinematic variables, since the multi-hadron contributions can be expressed as integrals over 2-particle intermediate states [6,7] while the elementary quark processes should be characterized by the QCD mass scale. We also expect T^{1PI}_{LIJ} to be small. Thus we choose to parametrize T^{1PI}_{LIJ}, along with meson-baryon vertex Γ, by smooth functions adjusted to fit the dependence of the observed scattering amplitudes on the kinematic variables s, t and u. We can interpret their dependence on these variables as expressions of the range and non-locality of the effective hadronic interactions [3].

While the effective vertices T^{1PI}_{LIJ} and Γ depend smoothly on the kinematic variables, the propagators have singularities corresponding to the existence of propagating-wave states. Furthermore the exchanged particles in Figure 2.1 occur off their mass shells. Thus we have to construct their propagators carefully.

The propagation of a particle is described in field theory by its two-point Green's function

$$G_{\alpha\beta}(x_1, x_2) \equiv < T\Phi_\alpha(x_1)\Phi_\beta(x_2) > - < \Phi_\alpha(x_1) >< \Phi_\beta(x_2) > \tag{2.2}$$

where $\Phi_\alpha(x_1)$ is the field operator for the component α (e.g. spin, isospin) of the field Φ at coordinate $x = (t, \mathbf{r})$, and T represents the Feynmann time ordering. In vacuum or uniform matter, translational invariance implies that G depends only on the relative coordinate $x_2 - x_1$. It is convenient to work with the Fourier transform of G, the propagator$D(p)$:

$$D_{\alpha\beta}(p) = i \int d^4x e^{ipx} G_{\alpha\beta}(0, x). \tag{2.3}$$

This dressed propagator is related to the non-interacting free-field propagator D^0 by the Dyson equation

$$D(p)^{-1} = D^0(p)^{-1} + \Sigma(p) \tag{2.4}$$

where Σ is the self-energy due to interactions. In addition to mean-field (Hartree) contributions, Σ contains vacuum-polarization loops in which the bare interaction causes the propagating particle to decay into two- and three-particle intermediate states [8] which then recombine via the dressed interaction, restoring the original particle. These loop contributions to the self energy are related to the Hartree tadpole by an exchange of internal and external fields. In vacuum the tadpole vanishes because the fields of all the low-mass hadrons carry quantum numbers of unbroken symmetries of the strong interaction (rotation, parity, flavor) and therefore have no vacuum expectation values; thus the vacuum self-energy is made up only of polarization loops.

The contribution to the self energy of the Δ from its decay into a nucleon by emitting a pion is shown in Figure 2.4. Dashed and solid lines are dressed boson and fermion propagators respectively. The shaded triangle represents the dressed proper three-point vertex Γ. The solid triangle represents the partially irreducible, proper three-point vertex Γ^I which has been corrected for overcounting as in equation (2.11) (after [6]). The Dyson equation (2.4) describes the mixing of these states with the bare Δ. The most striking result is that the Δ acquires a width due to the imaginary part of Σ . This width expresses the decay rate for the reaction $\Delta \rightarrow \pi N$, the inverse of the lifetime of the Δ.

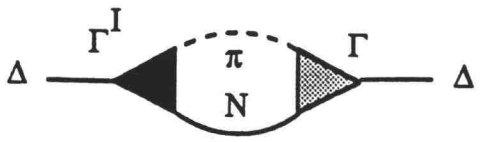

Figure 2.4. Contribution to the Δ self-energy due to its decay to a pion and a nucleon.

The corresponding self-energy Σ in the Dyson equation is given in terms of the decay vertex Γ_Δ by a loop integral. The imaginary part of the loop is determined by unitarity in terms of the imaginary parts of the pion and nucleon propagators [3]:

$$Im\ \Sigma(p) = -2 \int \frac{d^4q}{(2\pi)^4} \Gamma^I_\Delta(q, p-q) Im\ D_\pi(-q) Im\ D_N(p-q) \Gamma_\Delta(q, p-q)$$

$$\{\theta(p_0 - q_0)\theta(q_0) + \theta(q_0 - p_0)\theta(-q_0)\} \tag{2.5}$$

where the superscript I indicates an irreducible vertex which is related to the full vertex by an overcounting correction [6]. The second term in curly brackets corresponds to antinucleon intermediate states, and contributes only for $p_0 < 0$, i.e. for antideltas, in which case the first term vanishes. The vertices are spinor matrices connecting the spin-1/2 nucleons to the spin-3/2 deltas, and thus must be spin-1 vectors in their spatial dependence in order to conserve angular momentum. Causality then determines [3] the real part of the self-energy in terms of its imaginary part via the dispersion relation:

$$Re\ \Sigma(p) = Re\ \Sigma(p_0, p) = \frac{1}{\pi} P \int dp_0' \frac{Im\ \Sigma(p_0', p)}{p_0' - p_0}, \tag{2.6}$$

where $P\int$ means a principle-value integration. Causality also requires that the propagators obey an identical dispersion relation. We can thus concentrate on the

imaginary parts of the self-energy and the propagators, obtaining real parts from the dispersion relations when necessary. We follow this strategy both in our formalism and in our numerical computations. Our enforcement of causality in the delta propagation that distinguishes our treatment from other relativistic phenomenological models.

We choose the Rarita-Schwinger representation of the Δ, which embeds its spin S=3/2 in an $S = 1 \times S = 1/2$ space by representing it as a 4-vector of Dirac spinors $u^\mu_\epsilon(k, M^2)$. This representation is overcomplete, since the $S = 1 \times S = 1/2$ space also contains a spin-1/2 representation; when necessary we project into the spin-3/2 subspace using the projector [10]:

$$\Lambda^{\mu\nu}(p) \equiv \sum_\epsilon \overline{u}^\mu_\epsilon(p, p^2 = M^2) u^\nu_\epsilon(p, p^2 = M^2) \tag{2.7}$$

$$= g^{\mu\nu} + \frac{1}{3}\gamma^\mu\gamma^\nu - \frac{1}{3M^2}(\not{p}p^\mu\gamma^\nu + \gamma^\mu p^\nu \not{p}).$$

In this representation, the Δ propagator is a Lorentz tensor of spinor matrices $D^{\mu\nu}_\Delta(p)$, and the $\pi N\Delta$ vertex is given by

$$\Gamma^\mu_\Delta(q, p-q) = q^\mu \frac{f_\Delta}{m_\pi} F_\Delta(p^2, q^2, (p-q)^2)\mathbf{T}. \tag{2.8}$$

where $\mathbf{T}$ couples the isovector pion and the isospin-1/2 of the nucleon to the isospin-3/2 projection of the delta [9]. In vacuum, the form factor F_Δ is a Lorentz scalar and thus can depend only on the invariant masses p^2, q^2, and $(p-q)^2$ of the delta, pion, and nucleon respectively. The bare and dressed vertices both have the form of equation (2.8), differing only in the coupling constant f and the form factor F.

The Δ self-energy is also a Lorentz tensor of (isoscalar) spinor matrices $\Sigma^{\mu\nu}_\Delta(p)$. Constructed via equation (2.5), it will have spin-3/2 and spin-1/2 parts; since the vertex (2.8) conserves angular momentum, there is no coupling between the spins. After projection onto the spin-3/2 subspace, the self-energy may be expressed in terms of scalar and vector parts, both proportional to the projector Λ:

$$\Sigma^{\mu\nu}_\Delta(p) = \Lambda^{\mu\nu}(p)\{\Sigma^s_\Delta(p) + \not{p}\Sigma^v_\Delta(p)\} \tag{2.9}$$

This decomposition is unique, because $\Lambda^{\mu\nu}(p)$ commutes with $\not{p}$. The scalar function $\Sigma^s_\Delta(p)$ and the vector function $\Sigma^v_\Delta(p)$ each fulfill the dispersion relation (2.6), as

may be seen in the rest frame $\mathbf{p} = 0$ where $\Lambda^{\mu\nu}$ is independent of p_0, Similarly, the Δ propagator $D^{\mu\nu}_{\Delta}(p)$ may be expressed in scalar and vector parts, each proportional to the projector:

$$D^{\mu\nu}_{\Delta}(p) = \Lambda^{\mu\nu}(p)\{D^{s}_{\Delta}(p) + \not{p} D^{v}_{\Delta}(p)\} \tag{2.10}$$

Since the projector commutes with both scalars and Dirac vectors, the connection between the propagator and self energy is just like that for spin-1/2, once the self-energy has been projected into the physical spin-3/2 subspace.

To construct the delta self-energy from equation (2.5) we need not only the propagators of the intermediate pion and nucleon, but also the 3-field vertices Γ_{Δ} . Using the fully-dressed vertices to calculate the delta self energy would lead to overcounting of some of the rescattering contributions contained in the dressed vertex. This correction is accomplished by introducing the partially-irreducible vertex Γ^{I}_{Δ}, which differs from the full vertex by subtracting the part of the dressing due to two-particle πN intermediate states. The two-particle intermediate states can be removed by a rescattering equation [6], which relates the partially-irreducible vertex Γ^{I}_{Δ} to the full vertex:

$$\Gamma^{I}_{\Delta}(q, p_N) = \Gamma_{\Delta}(q, p_N) - \int \frac{d^4p}{(2\pi)^4} \Gamma^{I}_{\Delta}(q + p_N - p, p)$$

$$D_{\pi}(q + p_N - p) D_N(p) T^{1PI(s)}_{\pi N}(q + p_N - p, p; q, p_N) \tag{2.11}$$

where

$$T^{1PI(s)}_{\pi N} = T_{\pi N} - T^{1PR(s)}_{\pi N} = T^{1PI}_{\pi N} + T^{1PR(t)}_{\pi N} + T^{1PR(u)}_{\pi N} \tag{2.12}$$

is the nonresonant part of the πN scattering in the intermediate two-body πN state (resonant scattering would give a pole term in the self-energy, which would then lead to overcounting in the Dyson equation (2.4) for the propagator). Since this intermediate state has the quantum numbers of the delta, the non-resonant part $T^{1PI(s)}_{\pi N}$ is small. Thus we are justified in ignoring the overcounting corrections introduced by using the dressed 3-field vertex Γ_{Δ} to calculate the self-energy of the delta. Note that the two-body intermediate states also lead to a small imaginary part of the dressed vertex Γ_{Δ} when the delta's energy $(q + p_N)^2$ exceeds the πN

threshhold; this is just the imaginary part of the rescattering integral in (2.11), which we have argued is negligible. Indeed we have neglected the imaginary part of the vertex in constructing Im Σ via equation (2.5).

The procedure just described allows us to construct the dressed Δ propagator in terms of the bare mass M_Δ and the vertex strength $\frac{f_\Delta}{m_\pi} F_\Delta(p^2, q^2, (p-q)^2)$. Both these quantities have to be adjusted to fit the measured πN scattering. Since the Δ appears only in intermediate states, and since the form factor makes the dressing finite, it is not necessary to renormalize the delta; this is quite fortunate since no-one has succeeded in renormalizing a spin-3/2 particle.

In principle we also should dress the propagators of the other baryons and mesons, the most important of which are the nucleon and pion; since these appear in the initial and final states they ought also to be renormalized. However several investigations [10,11] have shown that, after renormalization, the propagators of the N and π are dominated by the on-mass-shell poles, with only small continuum strength in their cuts, which begin at threshholds of $M_N + m_\pi$ and $m_\pi + M_\rho$ respectively. In our work we have used only the physical-mass poles of all propagators except the Δ, taking the masses from the Particle Data Tables.

For s- and u-channel single-particle intermediate states, we must include the nucleon, delta, and the first excited state of the nucleon $N^*(\frac{1}{2}, \frac{1}{2})$ at 1.44 GeV, whose low-energy shoulder is apparent in the P11 phase shift above 1300 MeV. The resonence at 1.62 Gev (Δ^*) with isospin=3/2 and spin=1/2 is also included to account for S31 partial wave. All other non-strange baryons have greater masses and therefore are experimentally indistinguishable in our energy regime, from the smooth multiple-scattering contribution T^{1PI}. The lowest-energy t-channel single-particle state is the ρ, whose mass is so large that its exchange is practically indistinguishable from T^{1PI}; we include it, however, because of its significance for soft-pion theorem at threshold [9].

3. PHENOMENOLOGY

Our phenomenological program is now clear. We start with the known physical masses, plus an unknown bare mass for the delta. Corresponding to each s- and u-channel intermediate baryon β, we need to fit a 3-field vertex $\Gamma_{\pi N\beta}$ describing the coupling to the intermediate β. As discussed above for the $\pi N\Delta$ coupling, each vertex is given as the product of a local, zero range vertex Γ^0_β and a form factor F_β:

$$\Gamma_\beta = \Gamma^0_\beta F_\beta. \tag{3.1}$$

The local vertex contains the spin-isospin structure, while the form factor expresses the space-time extension of the hadrons. Similarly the t-channel ρ exchange requires two vertices, $\Gamma_{\rho NN}$ and $\Gamma_{\rho\pi\pi}$, each of which also may be factorized into a local vertex and a form factor. For convenience we use only one form factor F_ρ as the combination of the two form factors $F_{\rho\pi\pi}$ and $F_{\rho NN}$. All the local vertices used in our model are listed in Table 3.1.

Vertex	Local Part (Γ^0)
$\Gamma_{\pi_i NN}(x,y,z)$	$-i\frac{f}{m_\pi}\gamma^\mu\gamma_5\tau_i\frac{\partial}{\partial x^\mu}\delta(x-y)\delta(y-z)$
$\Gamma_{\pi_i N\Delta^\mu}(x,y,z)$	$\frac{f_\Delta}{m_\pi}\mathcal{T}_i\frac{\partial}{\partial x^\mu}\delta(x-y)\delta(y-z)$
$\Gamma_{\pi_i NN^*}(x,y,z)$	$-i\frac{f_{N^*}}{m_\pi}\gamma^\mu\gamma_5\tau_i\frac{\partial}{\partial x^\mu}\delta(x-y)\delta(y-z)$
$\Gamma_{\pi_i N\Delta^*}(x,y,z)$	$\frac{f_{\Delta^*}}{m_\pi}\gamma^\mu\mathcal{T}_i\frac{\partial}{\partial x^\mu}\delta(x-y)\delta(y-z)$
$\Gamma_{\rho_i^\mu NN}(x,y,z)$	$\{\frac{f_\rho}{2}\gamma^\mu+\frac{g_\rho}{4M_N}\sigma^{\mu\nu}\frac{\partial}{\partial x^\nu}\}\tau_i\delta(x-y)\delta(y-z)$
$\Gamma_{\rho_i^\mu\pi_j\pi_k}(x,y,z)$	$f_\rho\epsilon_{ijk}\delta(x-y)\frac{\partial}{\partial y^\mu}\delta(y-z)$

Table 3.1. Local Vertices in the Model

As was pointed out in our previous paper [12], this form factor in general is a function of three invariant distances, that is

$$F_\beta = F_\beta(x_{12}^2, x_{23}^2, x_{31}^2) \tag{3.2}$$

where x_{ij} stands for the space-time distance between particles i and j. It is more convenient to use its Fourier transfom:

$$F_\beta = F_\beta(p_1^2, p_2^2, p_3^2) \tag{3.3}$$

where p_i is the four momentum of particle i. In the lowest-order scattering, and also the Δ self-energy, all the vertices have two particles on-shell, leaving F_β as a function of the squared momentum of only one particle. This function is to be derived from experimental data.

As for scattering kinematics, all the quantities are expressed as functions of the Mandelstam variables, which are conveniently given in terms of the c.m. 3-momentum $\mathbf{q}$

$$s = {M_N}^2 + {m_\pi}^2 + 2\sqrt{{M_N}^2 + \mathbf{q}^2}\sqrt{{m_\pi}^2 + \mathbf{q}^2} + 2\mathbf{q}^2 \tag{3.4}$$

$$u = {M_N}^2 + {m_\pi}^2 - 2\sqrt{{M_N}^2 + \mathbf{q}^2}\sqrt{{m_\pi}^2 + \mathbf{q}^2} - 2\mathbf{q}^2 cos\theta \tag{3.5}$$

$$t = -2\mathbf{q}^2(1 - cos\theta). \tag{3.6}$$

We are faced with a problem which involves a large amount of data, namely six energy-dependent phase shifts and six different processes, each of which has a form factor to be fitted. One option is to carry out a large-scale computation and to determine the form factor via a best fit. The disadvantage of this strategy is that we may lose the chance to gain insight into the individual physical processes. Therefore we will instead focus on some specific features of the data and analyze relevant processes accordingly, so that we can pin down some of the parameters from each process.

Threshold behaviour is one of the features we will examine carefully, since there are quite accurate data for scattering lengths [9]. Around threshold the c.m. momentum is small, namely $\mathbf{q}^2 << M^2$, which enables us to expand all the quantities in term of $\mathbf{q}^2/M^2$. In an angular momentum projection procedure [13], we

carry out the expansion of the integrand and then derive the analytical expressions for scattering amplitudes due to each diagram for six partial waves. Thus we can calculate the contribution of each diagram to the scattering lengths of all the six partial waves: S11, S31, P11, P31, P13 and P33. In the Appendix we list expressions for the partial scattering lengths. We note that in the calculation form factors are set to 1 on mass shell.

3.1. P31 AND P13 PARTIAL WAVES

The most recent systematic investigation on low energy π-nucleon scattering is ref. [2]. One prominent feature of this theoretical analysis is that always $a_{13} = a_{31}$ at threshold and $K_{13} = K_{31}$ for the whole kinematic region. In contrast to this theoretical prediction, the experimental value of a_{31} is about 50 percent larger than a_{13}. With increasing energy, the ratio between the phaseshifts of P31 and P13 becomes about 2.2, and it keeps that value through almost the whole kinematic region under our investigation, (q=0–0.33 Gev) [14]. This discrepancy is due to the fact that the model [2] considers only processes with N, Δ and N^* as intermediate states. Clearly contributions from additional processes are needed. A simple discussion shows that the u-channel of N^*, Δ^* and seagull term (see subsection 3.3) are almost negligible, so that we need to consider only ρ exchange.

The ratio of the contributions from the ρ exchange to the P31 and P13 scattering lengths is determined by the ratio between the tensor and the vector part of the ρNN interaction, i.e. $\eta \equiv \frac{g_\rho}{f_\rho}$. This can be shown clearly at threshold: by using formulas (A.22-24) we derive the ratio as follows,

$$\lambda \equiv \frac{a_{31}(\rho)}{a_{13}(\rho)} = \frac{\eta(1+\frac{3m_\pi}{2M_N}) + (\frac{3}{4} + \frac{m_\pi M_N}{M_\rho^2} + \frac{3m_\pi}{8M_N})}{\eta - \frac{2m_\pi M_N}{M_\rho^2}} \cong \frac{1.22\eta + 1.02}{\eta - 0.44} \tag{3.7}$$

The ratio η has been investigated by many authors. Here we choose the analysis of Höhler and Pietarinen [15]. Via comprehensive considaration they derive the $\pi\pi \to N\overline{N}$ phaseshifts; then, with information about $e^+e^- \to \pi^+\pi^-$, they determined:

$$\frac{f_\rho^2}{4\pi} = 2.2, \quad \eta = \frac{g_\rho}{f_\rho} = 3.3. \tag{3.8}$$

With this choice of η, we have λ=1.76. We note that with energy increasing λ will become about 2.6 and it will stay almost constant for the whole kinematic region.

This phenomenon strongly suggests that the contribution from ρ exchange is dominant in the P31 and P13 channels. In other words, the N and Δ exchange contribution is suppressed by a drastically decreasing form factor for the u-channel as the crossed momentum transfer u goes farther off mass shell. With these qualitative features in mind we can design the form factor of ρ, N and Δ as follows

$$F_\rho(t) = \sqrt{\frac{\Lambda^4}{\Lambda^4 + (t - m_\rho^2)^2}}, \qquad \Lambda = 0.63\ GeV \tag{3.9}$$

$$F_{\pi N\beta}(Q^2) = [1 + \alpha_1 Q^2 + \alpha_2 Q^4] e^{-\sigma Q^4} \tag{3.10}$$

where β in the subscript stands for N, N^*, Δ and Δ^*, respectively, and

$$Q^2 = p^2 - M_\beta^2 \tag{3.11}$$

is the deviation of the transfered 4-momentum from the mass shell of the intermediate baryon β. We determine the u-channel form factors of $F_{\pi N\Delta}$ and $F_{\pi NN}$, and F_ρ by fitting the observed phaseshifts. We note that for $\beta = \Delta$ and N, a cubic term in the polynomial is needed and the coupling constants are so chosen that the form factor will be equal to one on mass shell.

The fitted phaseshifts for P31 and P13 partial waves are shown in Figure 3.1, where fitted are solid curves and data (represented by solid or open circles) are taken from [14]. The same signs are also used for Figures 3.2, 3.3, 3.5 and 3.6.

3.2. P33 AND P11 PARTIAL WAVES

It is obvious that the P33 partial wave is dominanted by the Δ resonance in the s channel. In the self-consistent calculation of the Δ self energy, the shape of the form factor $F_{\pi N\Delta}$ plays an essential role; in other words, the form factor can be well determined by fitting the P33 partial wave phase shifts. It is worth mentioning that the bare mass M_Δ is only about 30 MeV less than its observed mass.

The P11 partial wave is more complicated than P33, because there is an interplay among three processes : the s channels of N and N^* and ρ exchange.

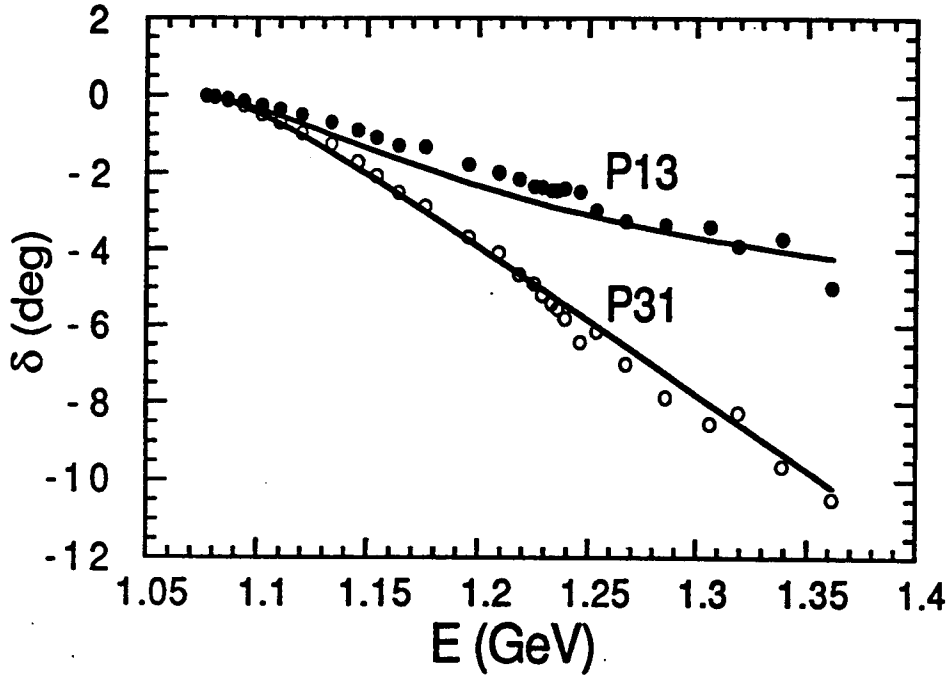

Figure 3.1. Phase shifts for P13 and P31 partial waves.

The resonance N^* is centered at $\sqrt{s}$=1.44 GeV beyond the high end of our energy region (1.36 GeV), therefore it plays a role only for the higher energy part of the region. The rapid increase of the phaseshift at higher energy is a reflection of that resonance. In the lower-energy region one can notice that the phase shift starts from the threshold with a trend going in the negative direction, then at around 1.15 Gev the trend reverses; around 1.22 Gev the phase shift crosses zero and increases steadily afterwards. This is a typical sign of the interference of two processes: the s channel of N, and ρ exchange. It is interesting to note that in the lower-energy region the phase shifts are very small, while the contribution from ρ exchange is not small (the form factor of ρ exchange is already determined by the P13 and P31 data). This requires a cancellation between N and ρ contributions, and therefore the form factor of N can determined with good precision.

The fitted phaseshifts for P11 and P33 partial waves are shown in Figure 3.2 and Figure 3.3, respectively. Figure 3.4 shows the imaginary part of the self-energy of the Delta resonance, with solid and dotted lines representing scalar and vector parts, respectively.

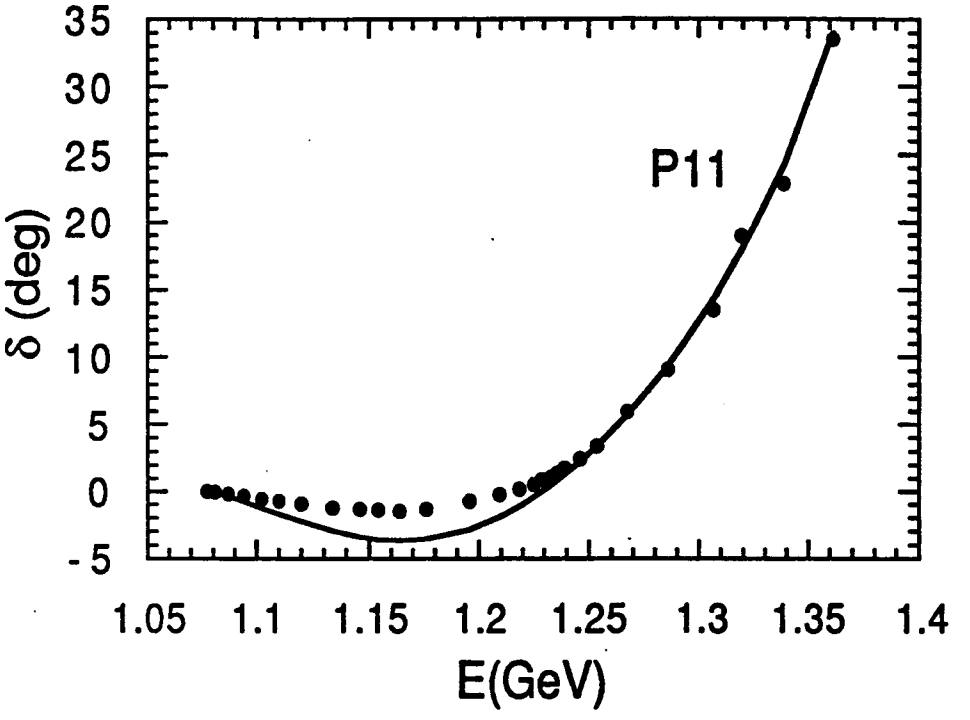

Figure 3.2. Phase shifts for P11 partial wave.

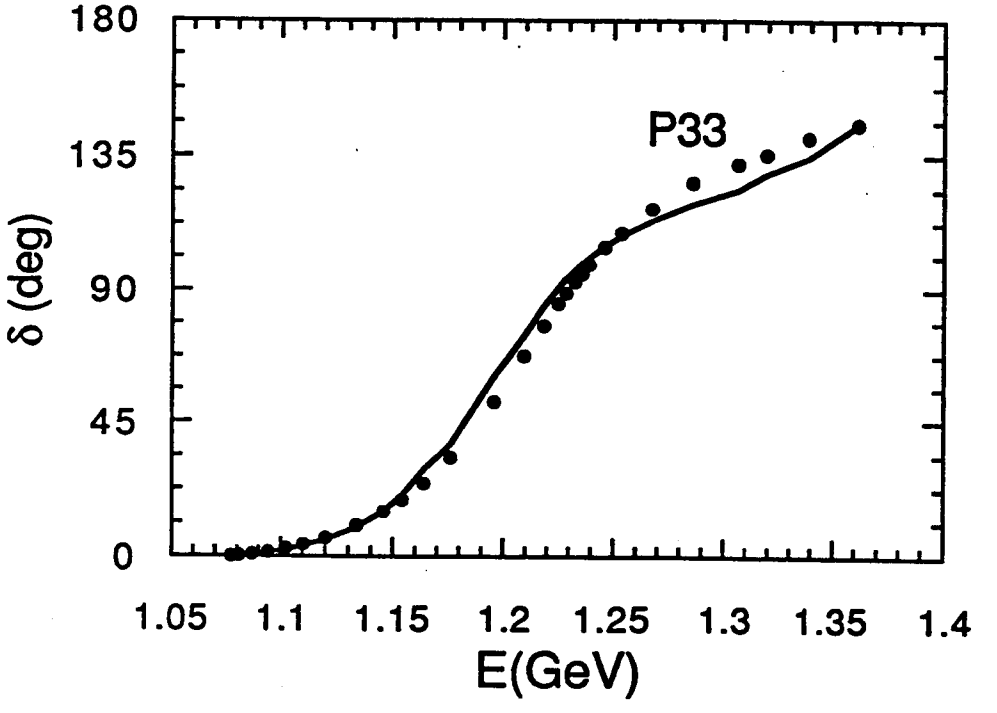

Figure 3.3. Phase shifts for P33 partial wave.

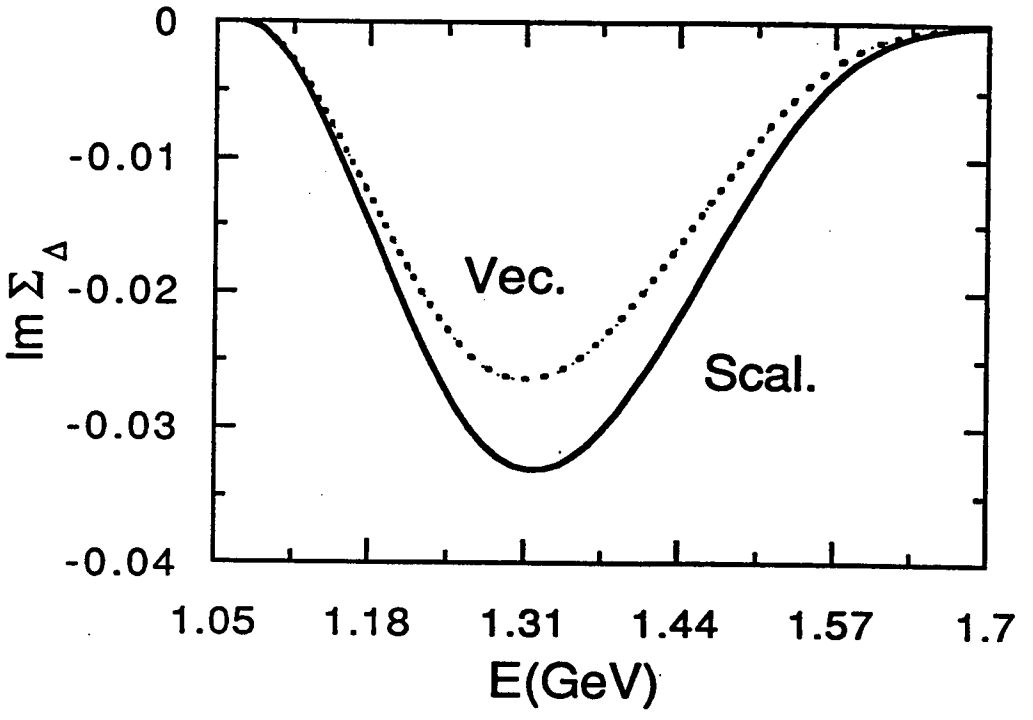

Figure 3.4. Scalar- and vector-part of the self-energy of Δ.

3.3. S-WAVE SCATTERING AND CHIRAL SYMMETRY

Up till now the only undetermined form factor is that of Δ^*. The quantum numbers of Δ^* are isospin=3/2 and spin=1/2, therefore its s channel should contribute to S31 partial wave only. The center of the Δ^* resonance is 1.62 GeV, far away from the high end of our energy region, so it should influence only the highest energy data points.

For S-wave scattering there is an important physical principle to be addressed, that is the chiral symmetry which causes a "seagull" term. The πNN interaction used so far breaks chiral symmetry. To restore chiral symmetry, Weinberg introduced the following Lagrangian [16]:

$$\mathcal{L}_W = \overline{\Psi}(i\gamma^\mu D_\mu - M_N)\Psi - i\frac{f}{m_\pi}\overline{\Psi}\gamma_5\gamma^\mu\tau\Psi D_\mu\pi - \frac{1}{2}D_\mu\pi D^\mu\pi - \frac{1}{2}{m_\pi}^2(1+\frac{\pi^2}{F_\pi^2})^{-1}\pi^2; \tag{3.12}$$

where Ψ is the nucleon field, and π is the pion field, τ is the isospin matrix and F_π=189 MeV is the pion decay constant. The covariant derivative in the Weinberg Lagrangian is given by

$$D_\mu \pi = (1 + \frac{\pi^2}{F_\pi^2})^{-1} \partial_\mu \pi \tag{3.13}$$

$$D_\mu \Psi = [\partial_\mu + i(F_\pi^2 + \pi^2)^{-1} \tau(\pi \times \partial_\mu \pi)]\Psi \tag{3.14}$$

Expanding $D_\mu \Psi$ and retaining terms up to order π^2, we obtain the zero-range πNN coupling of Table 1 and the seagull term of $\pi - N$ scattering,

$$\mathcal{L}_{seagull} = -F_\pi^{-2} \overline{\Psi} \gamma^\mu \tau(\pi \times \partial_\mu \pi)\Psi \tag{3.15}$$

This Lagrangian contributes to both s- and u-channel scattering diagrams; in each case its strength has to be modified by the same form factors as in the corresponding nucleon-pole diagram in order not to spoil the chiral symmetry. Figure 3.5 is a comparison between data and calculation for phaseshifts in S31 channel.

For the S11 partial wave there is no parameter to adjust, therefore, the extent of agreement between theoretical calculations and data can be taken as a check of the theoretical model and the form factors, which are already determined in other channels. From Figure 3.6 we can see that the agreement is impressive.

Figure 3.7 shows fitted s and u channel form factors of $F_{\pi NN}$, $F_{\pi N\Delta}$, $F_{\pi NN^*}$ and $F_{\pi N\Delta^*}$. The experimentally accessible regions for the s and u channels are shown as solid lines; the dashed lines are extrapolations using our fitted forms. Table 3.2 lists the parameters of the form factors determined by the above-mentioned procedure.

For all the channels unitarity is implemented by adding an adequate rescattering term, which is small in magnitude and dominately imaginary by nature. Figure 3.8 is the Argand diagram for the P33 partial wave. The circle is the unitarity line, and the open dots are our fits to the representative energies. The solid dots are corresponding amplitedes without the contribution from the rescattering process.

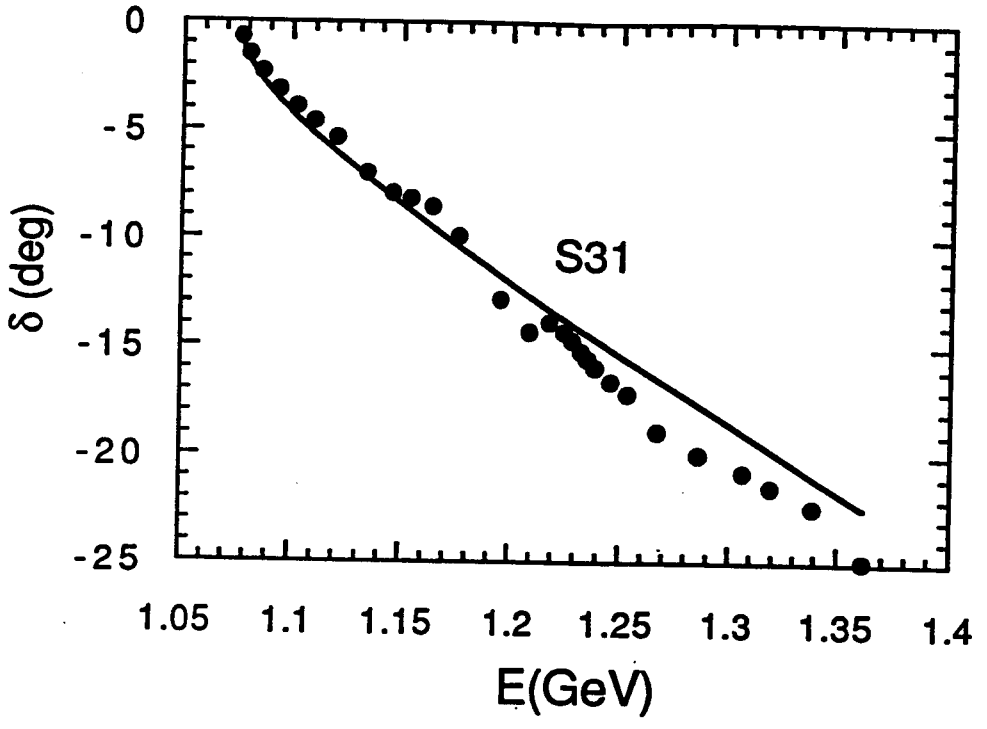

Figure 3.5. Phase shifts for S31 partial wave.

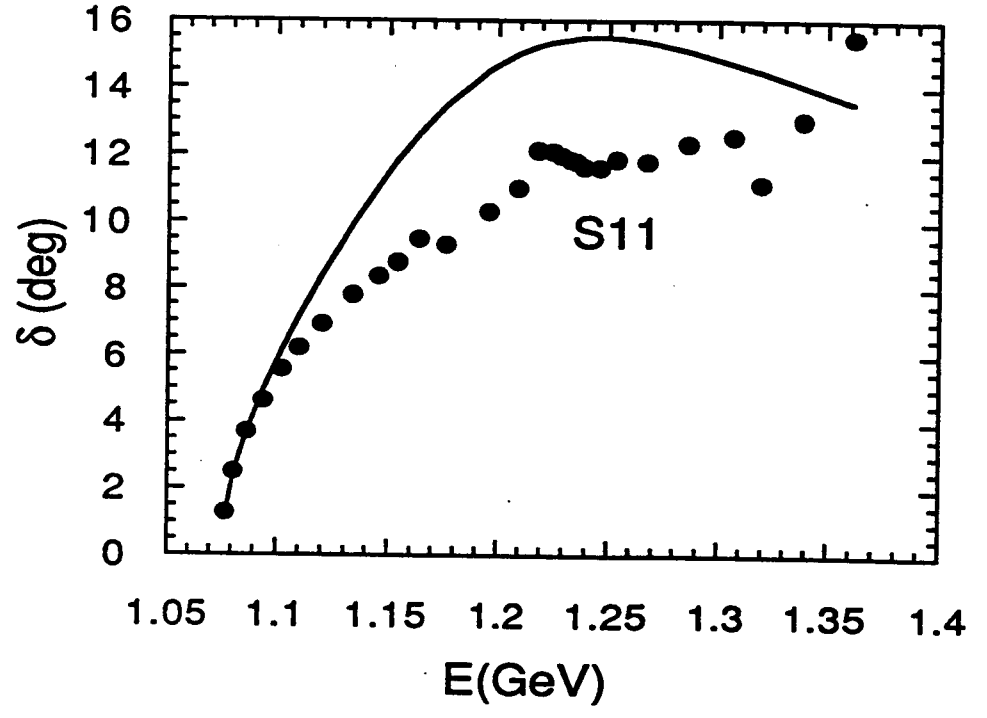

Figure 3.6. Phase shifts for S11 partial wave.

Vertex	Coupling Constants	α_1	α_2	α_3	σ
πNN	1.0	0.8	2.0	2.0	5.2
$\pi N\Delta$	2.1	-1.6	2.6	-0.8	4.5
πNN^*	0.27	0.5	0.4		1.2
$\pi N\Delta^*$	0.30	-0.2	0.3		0.9

Table 3.2. Fitted Parameters of Hadronic Form Factors

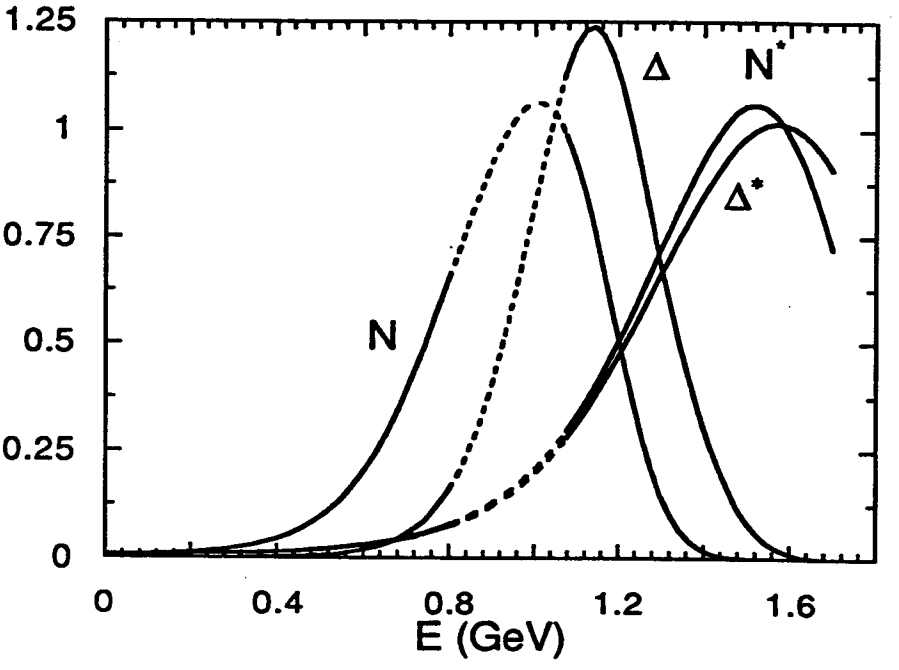

Figure 3.7. Fitted baryonic form factors $F_{\pi N\beta}$ for baryons β=N, Δ, N* and Δ^* as a function of the off-shell momentum transfer.

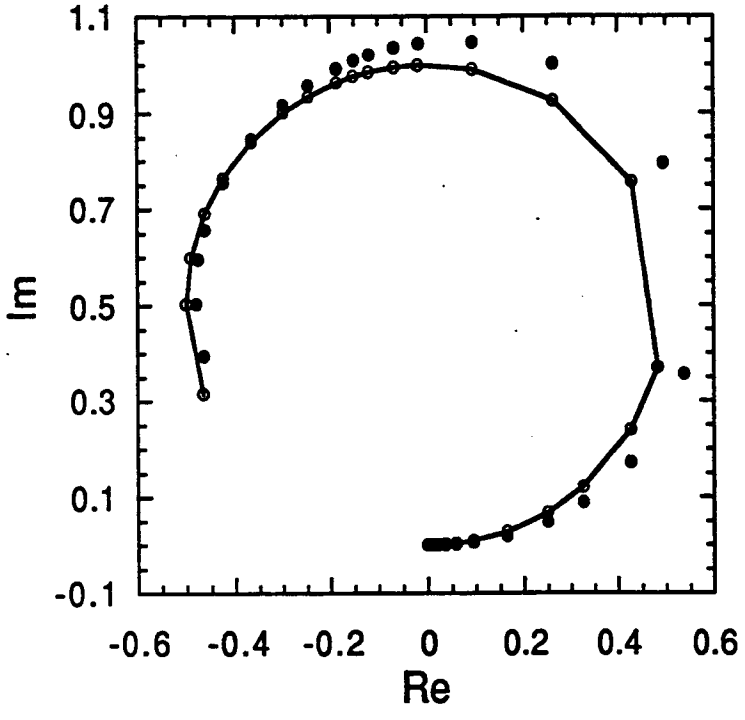

Figure 3.8. Argand diagram for resonant partial wave L=1, I=3/2, J=3/2.

4. RESULTS AND DISCUSSION

4.1. Δ RESONANCE AND SELF-CONSISTENCY

Our results can be understood in three ways. First, we have developed a covariant, unitary, causal representation of the delta self-energy. Second, we have transcribed the scattering data into the form of partially off-shell πNN, πNΔ, πNN* and $\pi N\Delta^*$ vertices. Third, we have an accurate, covariant, crossing-symmetric representation of pion-nucleon scattering data through the energy of the delta resonance.

Our model for the delta employs causality and two-body unitarity to construct the self-energy directly from the delta's decay vertex to an on-shell pion and nucleon. Because this vertex dominates the P33 πN scattering amplitude, it is very well determined by the data in exactly the kinematic region needed for the delta self-energy. The pion and nucleon in the intermediate state are taken off-shell by the dispersion relation (2.6) which is a consequence of causality [3]. By including πN scattering data up to $\sqrt{s} = 1.36$ GeV, we determine the form factor essentially completely: it has fallen almost to zero at that energy. This means that the dispersion integral for the real part of the self-energy is very well determined by the scattering data. Remarkably this real part vanishes at the peak of the resonance, which is essentially at the bare delta mass $M_\Delta = 1.235$ GeV. This is a little surprising since the shape of the delta's strength function, given by the imaginary part of its propagator, is skewed toward higher energies - on the low-energy side, it has to go to zero at the πN threshhold. That built-in skewing is compensated, in the πN scattering amplitude, by the early and rapid fall-off of the vertices' form factor, which apparently is peaked below the delta's mass shell (Figure 3.7). The effective coupling constant on the delta mass shell is $f_\Delta F_\Delta = 1.75$. The result that the delta strength is only 30 MeV shifted from its bare mass suggests that the delta may be dominated by a 3-quark state, with small dressing by pion-baryon states. This picture is in harmony with the observation that the delta fits well into the decuplet of the simplest constituent quark model.

The rapid fall-off of the $\pi N\Delta$ form factor was expected [3], since it is needed to cut off the rapid rise of the gradient coupling in the neighborhood of the threshhold. The rate of fall-off, mearured by σ, is about the same as for the πNN form

factor (compare Table 3.2 and Figure 3.7). The magnitude of σ corresponds to a non-locality of about 0.5 fm in the invariant distance between the baryons entering and leaving the vertex.

As a parametrization of πN scattering in the region of the delta resonance, our model gives a 20-parameter fit to six phase shifts in the c.m. energy region from about 1.10 to 1.36 GeV. With the extent of agreement shown in Figure 3.1, 3.2, 3.3, 3.5 and 3.6, this seems like a reasonably efficient parametrization.

Our model for the delta propagator and for the off-mass-shell behavior of the vertices can be used as input to study the propagation of deltas and pions in matter. There, all particles are off their mass shells, so additional extrapolations are needed. A simplified version of our model has been applied to nuclear matter, with striking results [17] which would be little changed by the quantitative model presented here.

4.2. THE ROLE OF ρ EXCHANGE

As we pointed out in section 3.1, the ratio between the tensor and the vector part of the ρNN interaction plays a key role in the whole procedure of determining the parameters. This ratio has been pursued from different reaction processes, e.g., $\pi\pi \to N\overline{N}$, $NN \to NN$ and $e^+e^- \to \pi^+\pi^-$ [15]. The results of these investigations are different, ranging from 2.25 to 5.15 (the value 1.85 from a simple ρ exchange model analysis is excluded), which will give $\lambda(= a_{31}/a_{13})$ ranging from 2.08 to 1.55. Although a different choice of the value for η will alter those form factors quantitatively, it is clear that the ρ exchange plays an important role in P-wave scattering as well as in S-wave scattering.

In section 3.2 we attribute the smallness of the phaseshifts in the low-energy part of the P11 partial wave to the cancellation between the crossed nucleon term and the ρ exchange. We note this is different from the assessment of Oset et al. [2], where this is due to the cancellation between crossed nucleon and N^* terms. We argue that the role of ρ exchange has been shown very important, therefore, neglect of ρ exchange is inappropriate.

BIBLIOGRAPHY

[1] J. Hamilton, "High Energy Physics", p193, ed. E.H.S. Burhop, Academic Press, New York, 1967

[2] E. Oset, H. Toki and W. Weise, Physics Reports, Vol.83, 281(1982)

[3] P.J. Siemens, M. Soyeur, G.D. White, L.J. Lantto, and K.T.R. Davies, Phys. Rev. C40, 2641(1989).

[4] J.P. Milana and P.J. Siemens, Phys. Rev. C43, 2377(1991).

[5] S. Mandelstam, Phys. Rev. 115, 1741, 1752(1959).

[6] A.P. Vischer and P.J. Siemens, Ann. Phys., in press.

[7] J.W. Van Orden, M.K. Banerjee, D.M. Schneider and S.J. Wallace, Phys. Rev. C23, 2157(1981).

[8] P.J. Siemens and A.P. Vischer, Ann. Phys. in press; see also A.P. Vischer, Ph.D. dissertation, Physics Department, Oregon State University, February 1992.

[9] T. Ericson and W. Weise, "Pions and Nuclei" (Oxford University Press, 1988).

[10] R.E. Behrends and C. Fronsdal, Phys. Rev. 106, 345(1957); H.T. Williams, Phys. Rev. C31, 2297(1985).

[11] L. Wilets, "Mesons in Nuclei" , M. Rho and D. WIlkinson, editors (North-Holland, Amsterdam, 1979) 791.

[12] P.J. Siemens, A.P. Vischer and H.C. Wu, Nucl. Phys. A, to be published

[13] S. Gasiorowicz, "Elementary Particle Physics", John Wiley and Sons, New York, 1966

[14] R. Koch and E. Pietarinen, Nucl. Phys. A336, 331(1980).

[15] G. Höhler and E. Pietarinen, Nucl. Phys., B95, 210(1975)

[16] S. Weinberg, Phys. Rev. 166, 1568(1968)
C.K. Au and G. Baym, Nucl. Phys. A236, 500(1974).

[17] L. Xia, P.J. Siemens and M. Soyeur, Nucl. Phys. A578, 493(1994)

APPENDIX

APPENDIX: FORMULAS OF PARTIAL SCATTERING LENGTHS

Notations used in this appendix:

$c_{11}(Ns), c_{31}(Ns)$: scattering lengths of S11 and S31 partial waves, contributed from nucleon s channel process, etc.

$a_{11}(\Delta u)$: scattering volume of P11 partial wave, contributed from the Δ u-channel process, etc.

$$\alpha = \frac{1}{8\pi}\frac{M_N}{M_N + m_\pi}; \quad s_0 = (M_N + m_\pi)^2; \quad u_0 = (M_N - m_\pi)^2 \tag{A1}$$

1) Intermediate state: N

<u>s-channel:</u>

$$a_{11}(Ns) = -\frac{3\alpha}{2{M_N}^2}(\frac{f_\pi}{m_\pi})^2[2M_N + (2M_N + m_\pi)(1 + \frac{4{M_N}^2}{s_0 - {M_N}^2})] \tag{A2}$$

<u>u-channels:</u>

$$c_{11}(Nu) = -2\alpha(\frac{f_\pi}{m_\pi})^2[2M_N + m_\pi(1 + \frac{4{M_N}^2}{u_0 - {M_N}^2})]; \tag{A3}$$

$$c_{31}(Nu) = -2c_{11}(Nu) \tag{A4}$$

$$a_{11}(Nu) = -\alpha(\frac{f_\pi}{m_\pi})^2\{\frac{1}{2{M_N}^2}[-2M_N + (2M_N + m_\pi)(1 + \frac{4{M_N}^2}{u_0 - {M_N}^2})]$$

$$+\frac{16}{3}\frac{{M_N}^2 m_\pi}{(u_0 - {M_N}^2)^2}\}; \quad a_{31}(Nu) = -2a_{11}(Nu) \tag{A5}$$

$$a_{13}(Nu) = -\frac{2}{3}\alpha(\frac{f_\pi}{m_\pi})^2\frac{8{M_N}^2 m_\pi}{(u_0 - {M_N}^2)^2}; \quad a_{33}(Nu) = -2a_{13}(Nu) \tag{A6}$$

2) Intermediate state: Δ

s-channel:

$$a_{33}(\Delta s) = -\frac{2\alpha}{3}(\frac{f_\pi}{m_\pi})^2\frac{M_\Delta + M_N + m_\pi}{s_0 - {M_\Delta}^2} \tag{A7}$$

u-channels:

$$c_{11}(\Delta u) = c_{31}(\Delta u) \;=\; 0 \tag{A8}$$

$$a_{11}(\Delta u) = -\frac{32\alpha}{27}(\frac{f_\Delta}{m_\pi})^2\frac{M_\Delta + M_N + m_\pi}{u_0 - {M_\Delta}^2}\frac{{M_N}^2 + {m_\pi}^2}{(M_N - m_\pi)^2} \tag{A9}$$

$$a_{13}(\Delta u) \cong a_{31}(\Delta u) \;=\; \frac{1}{4}a_{11}(\Delta u); \quad a_{33}(\Delta u) \;=\; \frac{1}{4}a_{13}(\Delta u) \tag{A10}$$

3) Intermediate state: N^*

s-channel:

$$a_{33}(N^*s) = -\frac{3\alpha}{2{M_N}^2}(\frac{f_{N^*}}{m_\pi})^2[(M_N + M_{N^*}) + (2M_N + m_\pi)(1 + \frac{(M_N + M_{N^*})^2}{s_0 - {M_{N^*}}^2})] \tag{A11}$$

u-channel:

$$c_{11}(N^*u) = -2\alpha(\frac{f_{N^*}}{m_\pi})^2[(M_N + M_{N^*}) + m_\pi(1 + \frac{(M_N + M_{N^*})^2}{u_0 - {M_{N^*}}^2})] \tag{A12}$$

$$a_{11}(N^*u) = -\alpha(\frac{f_{N^*}}{m_\pi})^2\{\frac{1}{2{M_N}^2}[-(M_N + M_{N^*}) + (M_N + M_{N^*} + m_\pi) \cdot(1 + \frac{(M_N + M_{N^*})^2}{u_0 - {M_{N^*}}^2})] + \frac{4}{3}\frac{(M_N + M_{N^*})^2 m_\pi}{(u_0 - {M_{N^*}}^2)^2}\} \tag{A13}$$

$$c_{31}(N^*u) = -2c_{11}(N^*u); \quad 31(N^*u) = -2a_{11}(N^*u) \tag{A14}$$

$$a_{13}(N^*u) = -\frac{2}{3}\alpha m_\pi(\frac{f_{N^*}}{m_\pi})^2\frac{2(M_N + M_{N^*})^2}{(u_0 - {M_{N^*}}^2)^2}; \quad a_{33}(N^*u) = -2a_{13}(N^*u) \tag{A15}$$

4) Intermediate state: Δ^*

<u>s-channel:</u>

$$c_{31}(\Delta^* s) = 2\alpha(\frac{f_{\Delta^*}}{m_\pi})^2[-(M_N + M_{\Delta^*}) + m_\pi(1 + \frac{(M_N + M_{\Delta^*})^2}{s_0 - {M_{\Delta^*}}^2})] \tag{A16}$$

<u>u-channel:</u>

$$c_{11}(\Delta^* u) = -\frac{8}{3}\alpha(\frac{f_{\Delta^*}}{m_\pi})^2[(M_N + M_{N^*}) + m_\pi(1 + \frac{(M_N + M_{\Delta^*})^2}{u_0 - {M_{\Delta^*}}^2})] \tag{A17}$$

$$a_{11}(\Delta^* u) = -\frac{4\alpha}{3}(\frac{f_{\Delta^*}}{m_\pi})^2\{\frac{1}{2{M_N}^2}[-(M_N + M_{\Delta^*}) + (2M_N + m_\pi)$$

$$\cdot(1 + \frac{(M_N + M_{\Delta^*})^2}{u_0 - {M_{\Delta^*}}^2})] + \frac{4}{3}\frac{(M_N + M_{\Delta^*})^2 m_\pi}{(u_0 - {M_{\Delta^*}}^2)^2}\} \tag{A18}$$

$$c_{31}(\Delta^* u) = \frac{1}{4}c_{11}(\Delta^* u); \quad a_{31}(\Delta^* u) = \frac{1}{4}a_{11}(\Delta^* u) \tag{A19}$$

$$a_{13}(\Delta^* u) = -\frac{8\alpha}{9}(\frac{f_{\Delta^*}}{m_\pi})^2\frac{(M_N + M_{N^*})^2 m_\pi}{(u_0 - {M_{\Delta^*}}^2)^2}; \quad a_{33}(\Delta^* u) = \frac{1}{4}a_{13}(\Delta^* u) \tag{A20}$$

5) ρ-exchange

$$c_{11}(\rho) = 2\alpha\frac{m_\pi}{{M_\rho}^2}f_\rho^2; \quad c_{31}(\rho) = -\frac{1}{2}c_{11}(\rho) \tag{A21}$$

$$a_{11}(\rho) = 2\alpha\frac{f_\rho}{{M_\rho}^2}[g_\rho(\frac{2}{3M_N} + \frac{m_\pi}{{M_N}^2}) + \frac{1}{2}f_\rho(\frac{4m_\pi}{3{M_\rho}^2} + \frac{1}{M_N} + \frac{m_\pi}{2{M_N}^2})] \tag{A22}$$

$$a_{31}(\rho) = -\frac{1}{2}a_{11}(\rho) \tag{A23}$$

$$a_{13}(\rho) = \frac{4}{3}\alpha\frac{f_\rho}{{M_\rho}^2}(-g_\rho\frac{1}{2M_N} + f_\rho\frac{m_\pi}{{M_\rho}^2}); \quad a_{33}(\rho) = -\frac{1}{2}a_{13}(\rho) \tag{A24}$$

6) Seagull Term

$$c_{11}(s.t.) = 8\alpha\frac{m_\pi}{F_\pi^2}; \quad c_{31}(s.t.) = -\frac{1}{2}c_{11}(s.t.) \tag{A25}$$

$$a_{11}(s.t.) = 2\alpha\frac{2M_N + m_\pi}{{M_N}^2}\frac{1}{F_\pi^2}; \quad a_{31}(s.t.) = -\frac{1}{2}a_{11}(s.t.) \tag{A26}$$

$$a_{13}(s.t.) = 0; \quad a_{33}(s.t.) = 0 \tag{A27}$$